Case Report

The role of diagnostic imaging and interventional radiology in liver schistosomiasis: A case report of advanced disease

Carmelo Cicciò [a,*], Giovanni Foti [a], Luigi Romano [a], Federico Gobbi [b], Eugenio Oliboni [a], Zeno Bisoffi [b,c], Giovanni Carbognin [a]

[a] *Department of Diagnostic Imaging and Interventional Radiology, IRCCS Sacro Cuore Don Calabria Hospital, Negrar di Valpolicella (VR), 37024, Italy*
[b] *Centre for Tropical Diseases, IRCCS Sacro Cuore Don Calabria Hospital, Negrar di Valpolicella (VR), 37024, Italy*
[c] *Department of Diagnostics and Public Health, University of Verona, Verona, 37134, Italy*

Abstract

Schistosomiasis is a neglected disease caused by trematode worms, affecting multiple target organs (predominantly the liver and urinary system) and presenting in wide spectrum including both acute and chronic forms; potential risks include liver fibrosis, portal hypertension, urinary tract obstruction, hydronephrosis, bladder cancer and reproductive tract disease. Diagnosis is mainly based on the evidence of infestation by parasitological, serological and molecular methods in body fluids (urine, stools and blood) and/or tissue specimens. Diagnostic imaging modalities (Ultrasonography, US; Computed Tomography, CT; Magnetic Resonance Imaging, MRI) support clinical-laboratoristic diagnosis with added value in evaluation of severity of morbidity and effectiveness of treatments. In most cases, early repeated anthelmintic chemotherapy can prevent the onset of advanced disease manifestations. Interventional radiology may offer an effective treatment option in case of variceal bleeding in advanced liver disease with portal hypertension resistant to conventional therapies.
© 2020 Beijing You'an Hospital affiliated to Capital Medical University. Production and hosting by Elsevier B.V. This is an open access article under the CC BY-NC-ND license (http://creativecommons.org/licenses/by-nc-nd/4.0/).

Keywords: Portal hypertension; Schistosomiasis; MRI; US; TIPS

1. Introduction

Schistosomiasis (Bilharziasis) is one of the most prevalent yet most neglected tropical diseases. It remains a serious public health problem in many subtropical and tropical developing countries, where there are approximately 230 million infected individuals. Many cases are found in Africa where more than 200,000 deaths are attributed to schistosomiasis annually. Approximately 700 million people worldwide are at risk of infection, and there is a high prevalence amongst inhabitants of sub-Saharan Africa, the Middle East and North Africa [1]. It is also an emerging health hazard in developed countries due to migratory flux, and it is increasingly reported among travellers returning from the tropics and other endemic areas.

The clinical course of schistosomiasis follows the life cycle of the parasite. Oviposition occurs concomitantly with, or immediately after, the acute phase [2], leading to the chronic phase of schistosomiasis. Severe and late manifestations of schistosomiasis may include cirrhosis with portal hypertension, splenomegaly, pulmonary hypertension and genitourinary disease (e.g. urinary strictures, hydronephrosis, bladder calcification). Most of the morbidity and mortality of hepatic schistosomiasis is due to upper gastrointestinal bleeding secondary to variceal rupture. Hepatocellular carcinoma and bladder cancer may develop in patients with chronic infection. However, these severe complications are associated with a high parasite burden. As such, they are frequently encountered

Please cite this article as: Cicciò C et al., The role of diagnostic imaging and interventional radiology in liver schistosomiasis: A case report of advanced disease, Radiology of Infectious Diseases, https://doi.org/10.1016/j.jrid.2020.03.007

in endemic populations but have rarely been described in travellers.

Schistosomiasis diagnosis is based on epidemiologic data, clinical manifestation, eosinophilia and evidence of living eggs at stool examination or serologic testing for schistosome infection. In the acute phase, laboratory tests can detect eosinophilia and an elevated level of immune complexes; however, a specific diagnosis can only be established using antibodies to the adult schistosome antigen.

Imaging diagnostic modalities are used in endemic areas as a non-invasive test, providing an alternative to invasive liver biopsy for diagnosis that can be used during active surveillance of liver chronic disease.

2. Case presentation

We report the case of a 39-year-old female, born in Madagascar, with a previous diagnosis of schistosomiasis, established 3 years before, who was admitted to our hospital due to episodes of diarrhoea and haematemesis with evidence of oesophageal varices. The previous diagnosis of schistosomiasis was based on microscopic evidence of *Schistosomiasis mansoni* eggs present in the stool.

At admission to our hospital, the patient showed signs and symptoms of chronic liver disease presenting with hepatosplenomegaly, ascites, and episodes of haematemesis/melaena. In addition, high-grade (F3) oesophageal varices were detected by oesophageal endoscopy. Laboratory findings revealed out-of-range values for: white blood cell (WBC), 4.5×10^9/L; red blood cell (RBC), 4.07×10^{12}/L; home communication terminal (HCT), 36%; platelet (PLT), 118×10^9/L; peripheric eosinophilia, 8.6%; s-albumin 32.78 g/L; s-alanine aminotransferase (s-ALT), 50 U/L; s-gamma glutamyl transferase (s-GGT), 58 U/L; total bilirubin, 21.4 μ mol/L (with normal direct bilirubin, 4.2 μmol/L); C-reactive protein of 26.3 mg/L. Normal levels of liver enzymes were observed and serologic tests for hepatitis virus (hepatitis B virus, HBV and hepatitis C virus, HCV) were negative. Anti-schistosoma antibody applied to serum samples, gave positive results; no circulating cathodic antigen (CCA) was detected in the urine sample and no eggs were found in faeces or urine samples. Given that the clinical evidence suggested no active disease, no anti-parasite treatment was undertaken.

2.1. Imaging findings

2.1.1. At admission

An ultrasound (US) showed hepatosplenomegaly and an inhomogeneous liver echostructure as evident by the hyperechoic thickened walls of portal venules (up to 7 mm) creating the "clay pipe-stem" pattern of periportal disease (Fig. 1A and B). Mild ascites was detected in the peritoneal cavity and dilatation of the portal and splenic veins. The portal vein was enlarged at the hilum (15 mm) and a hepatopetal portal flow was sampled by Color-Doppler (V_{mean}, mean velocity; 24 cm/s). No abnormal findings were detected at either the urinary tract or at other abdominal parenchyma.

2.1.2. During hospital recovery

Magnetic resonance imaging (MRI) was performed to allow an advanced evaluation of liver involvement, being preferred over Computed Tomography (CT) so as to avoid ionizing radiation exposure. MRI was performed using a high-strength field scanner (Avanto 1.5 T, Siemens Medical System, Erlangen, Germany) before and after i.v. administration of gadobenate dimeglumine (Gd-BOPTA), MultiHance, Bracco, Milan, Italy; 0.05 mmol/kg at a flow-rate of 2 mL/s followed by a 20 mL saline flush at 2 mL/s). The routine diagnostic MRI protocol included pre-contrast sequences (T1-weighted 2D-GE sequence in/out-phase, T2-weighted single-shot fast spin-echo (SS-FSE) sequence, T2-weighted with short-time inversion recovery, coronal T2-weighted half-Fourier turbo spin echo (HASTE) sequence, Echo-planar imaging-diffusion weighted imaging (DWI) sequence), dynamic contrast-enhanced T1-weighted 3D-GRE sequences with fat saturation (VIBE) were also used for the hepatobiliary phase. The determination of optimal scan delay for dynamic acquisition during material contrast administration, was achieved using the CARE Bolus technique (Siemens Medical Solutions, Erlangen, Germany) based on real-time monitoring of the bolus's arrival at the level of the vessel of interest, identified in our protocol as the suprarenal abdominal aorta. The optimal scan delay for late hepatic arterial phase was 17 s after the peak aortic enhancement. Portal venous, equilibrium and hepatobiliary phases were 70 s, 120 s and 75 min after Gd-BOPTA injection. The imaging protocol and technique parameters are described in table (Table 1).

SS-FSE and T2-weighted-STIR images showed periportal hyperintense thickening at the porta hepatis and around the intrahepatic branch (Fig. 2A); pseudonodular lesions with intermediate-high signal intensity around the periportal space were also detected in the same weighted images (Fig. 2B). These findings also showed a hyperintense signal at high b-value DWI sequences (Fig. 3A).

T1-weighted 3D-GRE images showed band-like hypo-intense and mild hyperintense pseudonodular lesions around the periportal space (Fig. 4A) both with marked enhancement after i.v. administration of gadobenate dimeglumine in the late arterial (Fig. 4B) and venous phase (Fig. 4C). No wash-out appearances were detected in the pseudonodular lesions at the portal and equilibrium phase, and no pathological hypo-intense lesions were detected in the hepatobiliary phase (Fig. 4D).

The apparent diffusion coefficient (ADC) value of liver parenchyma had a mean value of $0.94 \pm 0.03 \times 10^{-3}$ mm^2/s. Quantitative assessment of liver parenchyma was performed using open-source software (OsiriX Medical Imaging Software, Atlanta, GA, USA). ADC values of liver parenchyma were obtained from three standardized elliptical regions of interest (ROI; 1 cm^2) in right liver segments, initially positioned on the images obtained at b0 second/mm^2 (far from vascular, biliary channels and visible lesions) and then copied and pasted onto the corresponding location of the ADC maps (Fig. 3B).
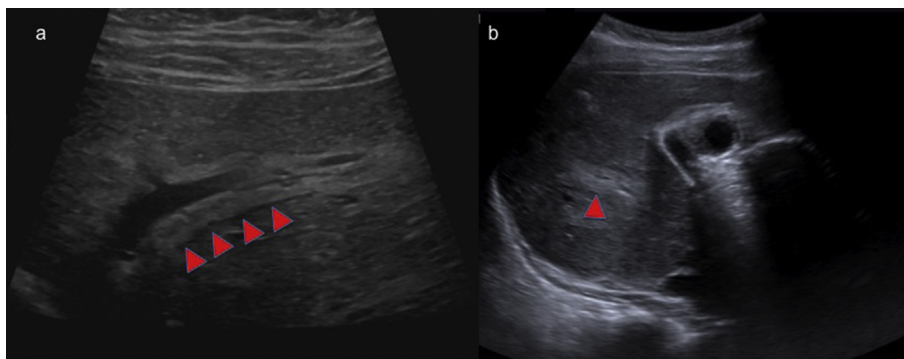
Fig. 1. Liver US (A—B). Increased echogenicity due to fibrotic bands was detected along the portal vein and its branch in the left (A; red arrowheads) and right lobes (B; red arrowhead).

Table 1
MRI protocol.

Parameter	T1wGE in/out	T2w SS-FFE	T2w-STIR	T2w HASTE	T1w GRE(VIBE)	DWI
Plane of acquisition	AXIAL	AXIAL	AXIAL	CORONAL	AXIAL	AXIAL
TR/TE (msec)	138/2.38−4.85	1000/91	1160/99 (TI 150)	1000/91	4.92/2,45	5300/78 (b-value 80 400 800 1000)
Flip angle (°)	70	160	150	145	10	90
ST/SG	5 3	5 3	5 3	5 3	3 3	5 6
NEX	1	1	1	1	1	4
RBW	390	710	710	710	345	1495
Phase direction	AP	AP	AP	AP	AP	AP
Echo-train length	2	102	104	149	1	57
Matrix	320 × 256	320 × 272	256 × 190	320 × 272	320 × 240	
FOV (mm)	360 × 360	360 × 360	360 × 360	400 × 400	360 × 360	274 × 360
Respiration	Breath-hold	Breath-hold	Breath-hold	Breath-hold	Breath-hold	-
Fat saturation	-	-	IR		Fat-Sat	-

Note. NEX: Number of Excitation; RBW: Receiver Bandwidth; FOV: Field of View; Fat-Sat, Spectral Selective Fat Saturation; IR: Inversion Recovery; TI, Time of Inversion; GRE or GE, Gradient Echo; VIBE, Volume Interpolated Breath-hold Examination; STIR, Short tau Inversion Recovery; SS-FSE Single Shot-Fast Spin Echo; ST, Slice Thickness; SG, Slice Gap; HASTE, Half-Fourier Single-shot Turbo-spin Echo; DWI, Diffusion-Weighted Imaging.

Morphological evaluation of the liver showed a rounded margin, with regional changes of morphology as seen in advanced liver disease, with segmental atrophy affecting the VI, VII and V segments of the right lobe. Segmental hypertrophy also involved the caudate lobe, II, III e IV segments with a caudate/right lobe ratio of 1.13. Images were both qualitatively and quantitatively evaluated for the presence of an enlarged periportal space. For the qualitative analysis, enlargement of the periportal space was subjectively evaluated by means of visual inspection; for the quantitative analysis, it was decided to estimate periportal thickness on STIR-T2 weighted images, at the hilum level and along proximal lobar branches where the vascular signal void was clearly seen to be within the plane of the axial image. The values of periportal thickness were 9 mm at hilum level and 5 mm along both side branches (measurements not shown). Liver volume was estimated as the product of multiplication of three perpendicular axes, measured on T1-weighted 3D-GRE sequences—caudocranial (12 cm) × latero-lateral (19 cm) × antero-posterior (14.5 cm) × 0.31 (correcting coefficient)—resulting in a three-dimensional value of 1025 cm^3 [3]. Splenic index (SpI) was estimated as the
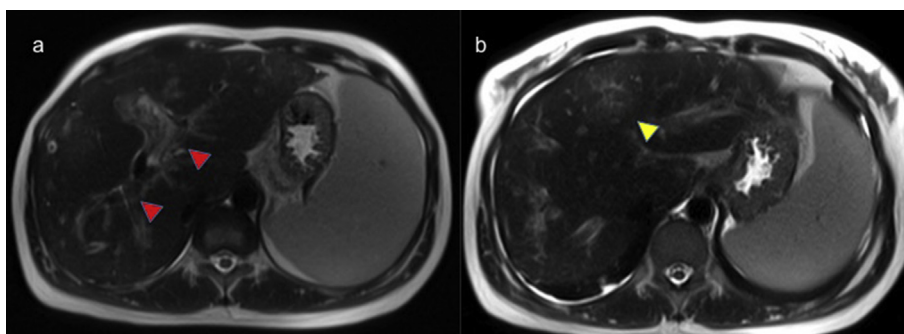

Fig. 2. Liver MRI (A, B). Axial T2w SS-FSE sequence MR images showed bands with high signal intensity, keeping with extensive periportal fibrosis (A; red arrowheads) and a pseudonodular lesion with high-intermediate signal intensity in the periportal space (B; yellow arrowhead).
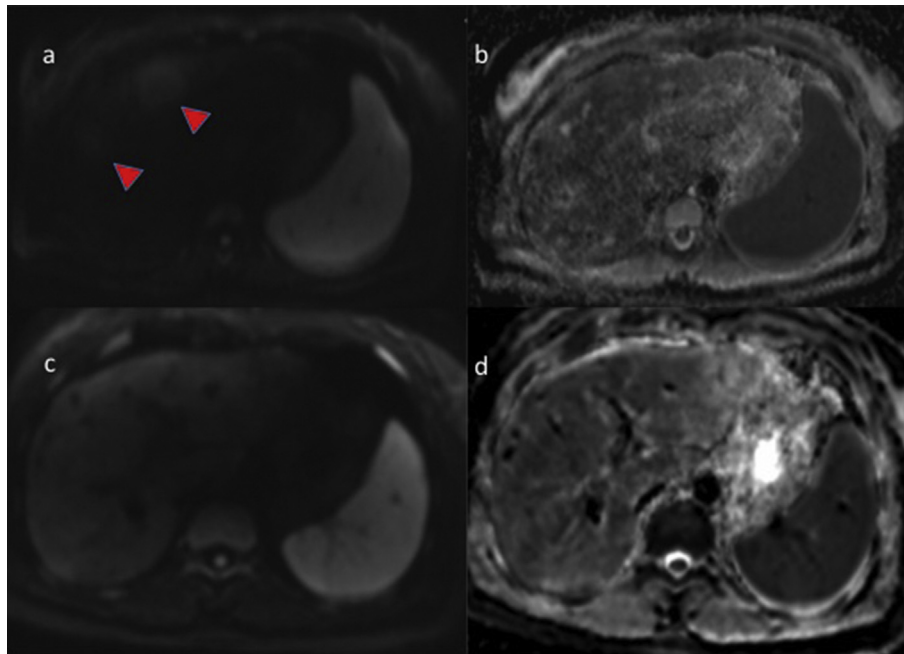
Fig. 3. Liver MRI (A−D). Comparison of DWI images (b-value: 800 s/mm^2) and corresponding ADC maps at hospital admission (A−B) and after 18 months (C−D).

product of multiplication of three linear dimensions, measured on T1-weighted 3D-GRE sequences—Maximal Length (14 cm) × Hilum Thickness (6.5 cm) × Vertical Height (14.5 cm)—resulting in a three-dimensional value of 1319 cm^3. Splenic volume (SV) was calculated using the three linear dimensions obtained in the formula: SV = 30 + 0.58 (Vertical Height × Hilum Thickness × Maximal Length) giving a value of 795 mL [4]. No siderotic nodules were detected.

2.2. Treatment

Three days after admission, given the ineffectiveness of endoscopic and medical attempts to control variceal bleeding, a transjugular intrahepatic portosystemic shunt (TIPS) procedure was performed to treat portal hypertension. A low-resistance channel was created between the right supra-hepatic vein and the right intrahepatic portal vein, and the tract
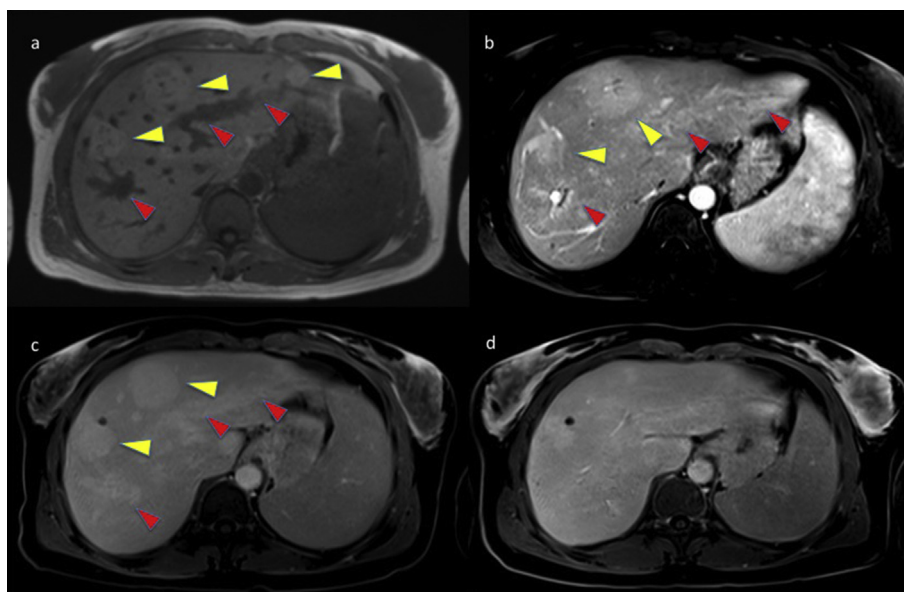

Fig. 4. Liver MRI (A−D). A, T1w 2D-GE sequence showed hypointense periportal fibrosis (red arrowheads) with hyperintense regenerative nodules (yellow arrowheads) around the periportal space; B−C, T1w 3D-GRE sequence (VIBE) showed a marked enhancement of periportal fibrosis and regenerative nodules in the late arterial and venous phases; D, no pathologic hypointense lesions were detected in the hepato-biliary phase.

was kept patent with deployment of an expandable metal stent across the two vessels (Fig. 5).

2.3. Follow-up

Clinical data: 18 months later, physical examination revealed tenderness in the right upper quadrant when palpated but no clinical evidence of splenomegaly or scleral icterus. Abnormalities were detected by laboratory findings for: WBC, 3.5×10^9/L; RBC 3.76×10^{12}/L; haemoglobin (HGB) 112 g/L; peripheric eosinophilia, 14%; s-albumin 36.8 g/L; s-ALT 50 U/L; s-GGT 58 U/L. Normal values for total bilirubin, 12.2 μmol/L and direct bilirubin, 2.2 μmol/L were observed. No eggs were found in either faeces or urine samples.

2.3.1. Imaging findings

US with Color-Doppler sampling (Fig. 6) was performed to verify shunt patency, showing phasic and hepatopetal flow in the main portal vein (V_{max} 35.5 cm/s; V_{mean} 30 cm/s; Fig.) with a mild decrease in diameter (13 mm vs 15 mm at admission) and a mild increase in the resistive index in the hepatic artery (RI 0.76, n.v. 0.55−0.7; Fig.) being detected. Color-Doppler US also showed the normal positioning of the device between the right portal vein and the right suprahepatic vein (Fig. 6A). Normal functioning of the TIPS device was apparent from the anterograde and hepatopetal flow through it from the caudal (near right portal vein; Fig. 6B), to middle (Fig. 6C) to cephalic portions (near connection of right suprahepatic vein to the inferior cava vein; Fig. 6D). No abnormal increase of peak flow velocity was detected in the device (Peak Velocity < 190 cm/s). MRI was performed using a high-strength field scanner before and after i.v. administration of Gd-BOPTA with the same imaging protocols used for the previous examination, even in the hepatobiliary phase. T2w-SS−FSE showed significant qualitative regression of periportal hyperintense thickening (Fig.7A) and a decreased measurement value at quantitative evaluation, as previously defined (periportal thickness at hilum was of 4 mm while around proximal side branches decreased to 2−3 mm;

Fig. 5. TIPS deployment between the right portal branch and right suprahepatic vein (yellow arrowhead).

measurements not shown); no pseudonodular lesions with hyperintense signal on DWI were detected around the periportal space (Fig.3C); T1-weighted 3D-GRE sequences (VIBE) demonstrated a reduction of periportal thickening (Fig. 7B) with mild and thin band-like enhancement along the periportal space and no evidence of pseudonodular enhancing lesions (Fig. 7C). No hypointense lesions were detected with features indicating high-risk lesions, in the hepatobiliary phase (Fig. 7D). Quantitative analysis of ADC values for liver parenchyma was performed, as previously defined, giving a mean ADC value of $1.13 \pm 0.09 \times 10^{-3}$ mm^2/s (Fig. 3D).

Liver volume was estimated, as previously defined, by measuring its maximum dimension in three perpendicular axes: caudocranial (10 cm) × latero-lateral (18 cm) × antero-posterior (14 cm) × 0.31, resulting in a three-dimensional value of 781 cm^3. As previously defined, SpI and SV were calculated from three linear splenic dimensions: Maximal Length (12 cm) × Hilum Thickness (6 cm) × Vertical Height (12 cm), resulting in an SpI of 864 cm^3 and an SV of 531 mL.

3. Discussion

Schistosomal splenohepatopathy, usually caused by *S. mansoni* infection, is a common form of chronic disease, characterized by organomegaly and hepatic fibrosis in the first stage, with signs and symptoms of portal hypertension in the later phase. While, in addition to other signs and symptoms, hepatosplenomegaly can be observed during acute schistosomiasis (also known as "Katayama fever"), schistosomal hepatopathy is considered to be a specific form of liver fibrosis, also known as "clay pipestem", portal or periportal fibrosis that is observed in the first stage of chronic disease. In particular, periportal fibrosis is a pathognomonic sign of liver schistosomiasis disease and is related to haemodynamic alterations of the portal system due to a granulomatous inflammatory reaction around entrapped eggs in the liver. Signs and symptoms of portal hypertension along with ascites, gastrointestinal variceal bleeding, severe anaemia and hypoalbuminemia are observed in the later phase, whereas hepatocellular carcinoma can manifest in advanced liver disease.

US is considered a reliable tool for the diagnosis of hepatosplenic disease in comparison to other clinical methods, having a high accuracy in the detection of periportal fibrosis and signs of portal hypertension (enlargement of the portal/splenic veins and patency of portosystemic collaterals) during chronic disease [5]. Furthermore, as an alternative to invasive liver biopsy, US is commonly used as a non-invasive diagnostic test in endemic areas. In an adjusted clinical context, US findings of echogenic areas around portal branches ("claypipestem" pattern) and gallbladder wall fibrosis, are considered pathognomonic of *S. mansoni* infection thus avoiding the need for liver biopsy [6]. Different and/or combined US-patterns of periportal fibrosis can be described upon US examination, using Niamey's classification [7]. Furthermore, US helps to assess the degree of periportal disease by measuring portal tract thickness (Grade I: 3−5 mm; Grade II: 5−7 mm; Grade III ≥ 7 mm), which reflects haemodynamic changes and
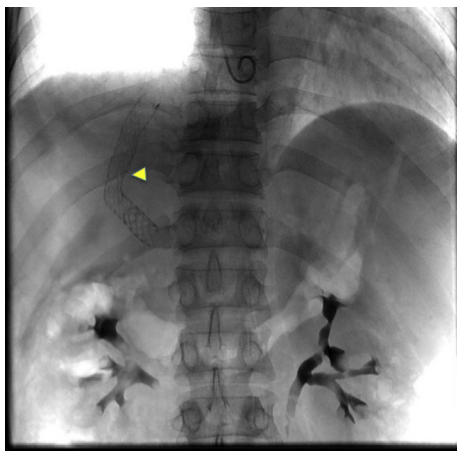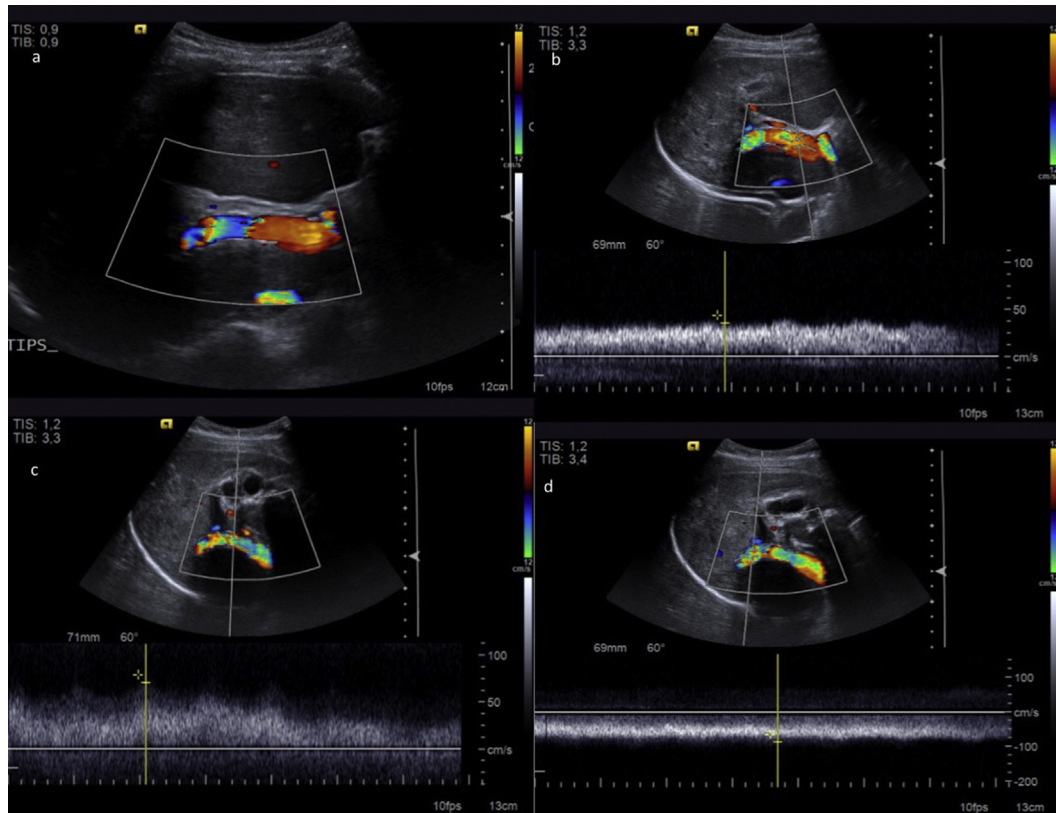
Fig. 6. Liver Color-Doppler US (A−D). A, Color-Doppler US showed the normal positioning of the device between the right portal vein and the right suprahepatic vein. B-D, normal functioning of the TIPS device was apparent from the anterograde and hepatopetal flow through it from the caudal to middle and finally to cephalic portions.
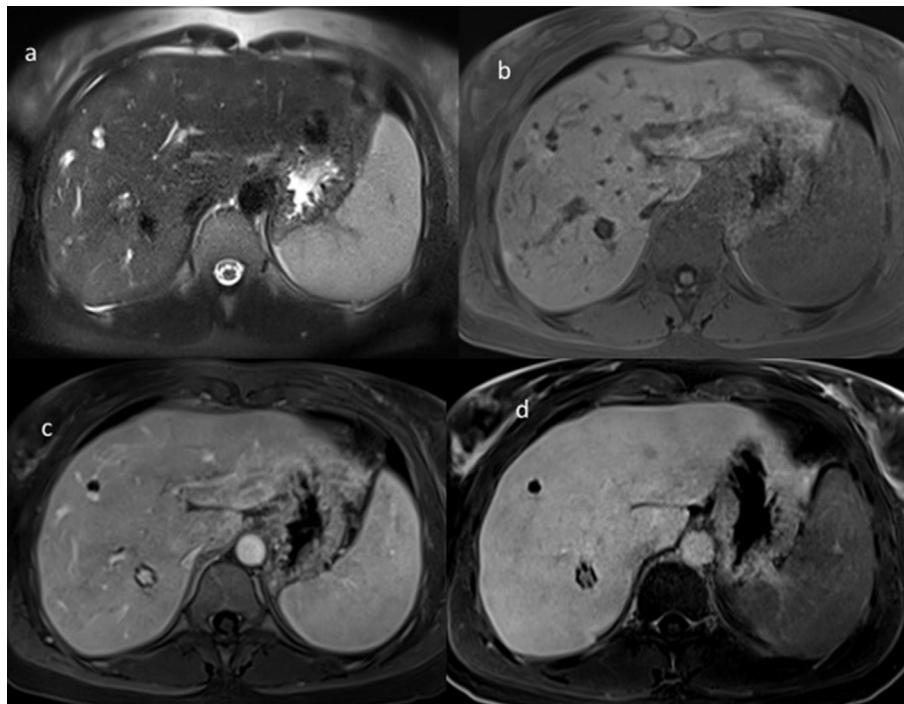

Fig. 7. Liver MRI (A−D). A, at 18 months, STIR-T2w images showed a reduction of hyperintense periportal bands with poorly defined pseudonodular lesions in the right lobe; B, T1WI 2D-GE sequences showed a decrease in the hypointense bands-like of periportal fibrosis and a net reduction in the size of large regenerative lesions with remnants of periportal areas with poorly defined hyperintense signal. C, a significant reduction of contrast enhancement was observed around portal tracts and along the sides of periportal bands in the venous phase; D, no pathologic hypointense lesions were detected in the hepatobiliary phase.

provides a good estimate of the clinical status of patients [7]. Other US findings included in the spectrum of chronic disease ("Symmers' fibrosis") are: splenomegaly, left liver lobe enlargement, right liver lobe reduction, portal vein tract dilatation, hepatofugal collateral circulation and portal thrombosis. At admission of the patient to our hospital, signs and symptoms of advanced liver disease with no other aetiology, eosinophilia and a typical appearance of the liver at ultrasound, were considered diagnostic of advanced schistosomiasis-related disease and, therefore, liver biopsy was not required.

Variceal bleeding is the most frequent lethal complication of liver schistosomiasis but neither clinical nor parasitological parameters are reliable prognostic indicators for the risk of haemorrhagic events. The use of an US score, computed by combining the degree of periportal thickening and size of portal vein, according to a *S. mansoni* sonographic score, might predict the risk of variceal bleeding in patients with periportal fibrosis due to *S. mansoni* infection. An increase in the diameter of the portal vein is associated with an increased risk (20%−35%) of bleeding from oesophageal varices and suggests a future risk of repeated bleeding (approximately 33%) even after antiparasitic treatment and endoscopic sclerotherapy [8,9].

There is evidence of regression of fibrosis and portal hypertension after treatment of schistosomiasis; however, limited data of US-regression of fibrosis is reported. Cota et al. studied 84 patients with hepatosplenic schistosomiasis from an endemic area, 4 years after treatment with oxamniquine, observing a regression of liver fibrosis in 32% of patients and reduction of splenomegaly in 48% of patients [10].

Color-Doppler-US increases the accuracy of US, providing data about physiopathological changes in portal circulation due to liver fibrosis (portal patency, direction of blood portal flow and evidence of hepatofugal circulation). Furthermore, it is a reliable tool in assessing the patency of a TIPS device, which may be deployed in the management of complicated portal hypertension.

CT, which was not performed in this case, is a well-established method used in the assessment of liver diseases. In patients with acute or chronic schistosomiasis, it defines morphological changes of liver lobes (both global or lobar liver enlargement or atrophy) and peculiar patterns of calcification (septal or capsular) in response to eggs. Periportal fibrosis is correctly depicted with typical periportal hypodense bands, with strong enhancement after iodine contrast agent administration. CT may demonstrate hypodense liver lesions that are occasionally reported in some cases of Katayama Syndrome. The use of ionizing radiation in CT may limit its use in favor of non-ionizing radiation techniques (e.g. MRI and US), at admission and during follow-up. However, CT should be considered in some cases due to its increased accuracy in evaluating co-existing extrahepatic manifestations of schistosomiasis (e.g. lung, bowel and urinary tract) [11].

MRI is a well-established method for the imaging assessment of the liver on account of its effectiveness in the evaluation of focal or diffuse liver disease. In the chronic phase of liver schistosomiasis, the morphologic alterations and periportal pattern of enhancement identified by MRI are highly reproducible and may provide reliable information regarding disease stage, progression and response to therapy.

In hepatosplenic schistosomiasis, common MRI features include heterogeneity of signal intensity of hepatic parenchyma, presence of peripheral vessels, periportal fibrosis, splenomegaly with siderotic nodules and dilated venous collateral vessels [12]. The most specific MRI finding in schistosomiasis is the altered appearance of periportal spaces, due to periportal fibrosis, which appear as hyperintense bands in T2-weighted images and as hypointense bands along portal vessels in T1-weighted images with increased signal intensity after paramagnetic material contrast administration, even in the delayed venous phase. Periportal fibrosis is crucial for evaluation of the disease stage and the success of treatment.

The significance of MRI in the evaluation of periportal fibrosis in schistosomiasis has not yet been fully determined as imaging data regarding the potential role of MR with multi-parametric imaging (basal MRI imaging; multiphasic contrast-enhanced magnetic resonance imaging, CE-MRI; DWI) are limited in the non-invasive characterization of periportal fibrosis with and without active inflammation and oedema. Basal MRI periportal hyperintensity on T2-weighted images is a robust imaging marker of combined oedema and inflammatory changes in active disease; nevertheless, in patients in chronic phase, mild hyperintense bands on T2-weighted images are detected, probably due to residual inflammatory periportal components [12]. At CE-MRI, the pattern (homogenous/patchy/linear) of liver contrast enhancement after gadolinium material contrast administration, assessed during early or late phase, is reported to help the differentiation between active and chronic disease. This evidence is generally investigated in pathologically established chronic hepatitis attributed to causes other than schistosomiasis, in which an earlier, patchy pattern is associated with active hepatocyte damage and inflammatory infiltration while a later, linear pattern is consistent with extracellular fibrosis [13]. In liver schistosomiasis, while the significance in the pattern of early gadolinium enhancement has not yet been fully investigated, it has been noted that pathogenesis of liver schistosomiasis is related to an immune response to egg deposition with granuloma formation rather than pure hepatocyte damage which is observed in chronic hepatitis due to common aetiologies. Neoangiogenesis and obstructive vascular lesions due to portal fibrosis, induce alterations in liver haemodynamics with a reduction in venous portal flow and parenchymal arterialization to which early pattern of enhancement may deal with. In our case, a linear pattern of enhancement was detected during early phase with a reduction of its entity at the MRI examination performed during follow-up. As such, large regenerative nodules (LRG), previously unreported in a similar clinical setting, may be considered hyperplastic/hypervascular lesions caused by vascular derangements in arterialized parenchyma [14]. More robust is the association between the late pattern of liver enhancement and fibrosis with late retention of gadolinium in advanced disease, observed too in our case, resulting

from the expansion of the extracellular compartment due to fibrosis. Hepatobiliary-specific contrast agents have an important diagnostic role in advanced and chronic liver disease in the detection and characterization of focal high-risk borderline nodules as high-grade dysplastic nodules (DN) or as early hepatocellular carcinoma (HCC), having a direct impact on the optimization of follow-up imaging or biopsy. Furthermore, in chronic liver disease, expression and function of the hepatocyte transporters is often impaired, resulting in a decrease of hepatic enhancement on hepatobiliary phase images. The uptake of these agents by the liver tissue also relates to hepatocyte function and therefore has been investigated as an alternative approach to the evaluation of liver function and diffuse liver disease [15]. DWI is a widely available MR technique that measures the microscopic motion of water, classically called Brownian motion and is measured in terms of apparent diffusion coefficient (ADC; mm^2/sec); this value is obtained using a monoexponential model, with as few as 2 data points, generally 1 without motion-encoding gradients ($b = 0$ s/mm^2) and 1 with high diffusion weighting ($b = 200$ s/mm^2); ADC values result from the slope of a linear regression of the semi-log data. Some studies have reported a decrease of the ADC values with increasing liver fibrosis in comparison to healthy controls and it has been hypothesized that it could be explained by a restricted diffusion effect related to the deposition of glycosaminoglycans, proteoglycans and collagen fibres in the diseased liver. However, there are some concerns about the use of DWI in the staging of liver fibrosis in light of robust evidence that the ADC measurement in liver fibrosis reflects perfusion abnormalities rather than real restricted water diffusion related to an increase of extracellular matrix [16]. This hypothesis has been further tested using the Intravoxel Incoherent Motion (IVIM) technique, a promising developed DWI-derived approach that can separate the effects of perfusion-related diffusion from the pure random microscopic motion of water molecules [17]. IVIM analysis is performed using several b-values, in particular with low b values (< 200 s/mm^2) and data is analysed using a biexponential model to obtain 3 parameters: D, or the diffusion coefficient (slow component of diffusion), D*, or the perfusion or pseudodiffusion coefficient (fast component of diffusion) and Pf, the perfusion fraction of microcirculation. The role of DWI-ADC-IVIM is complex also on account of several potential confounding factors that may impair a reliable correlation between diffusion and liver fibrosis as technical parameters (e.g. field strength, repetition time, echo time and b-values) also with hepatic steatosis, hepatic iron, liver inflammation that may coexist in chronic liver disease. Although the use of IVIM is very appealing in the case of liver fibrosis evaluation [17], conflicting results have been reported with limits in detecting early stage of liver fibrosis and diagnosing liver fibrosis grades. The main concern is an unsatisfactory reproducibility of results of scan-rescan quantification of the perfusion compartment of D* and Pf, with low sensitivity of D to pathological change [18]. As observed by others and also in our case, the role of DWI in liver fibrosis evaluation remains unclear. The ADC value sampled in liver

parenchyma at admission was lower than observed 18 months later, seemingly as an effect of the improved free-motion of water protons. It could be postulated, as observed in other studies, that a potential role of modification of perfusion status of the liver, related to a reduction of perfusion abnormalities due to a decreased effect of periportal fibrosis also with the complex impact of the TIPS procedure used to correct portal hypertension.

MRI reproduces the pathological findings of Symmers' fibrosis more reliably than other imaging techniques, without the risks associated with radiation exposure (as compared to CT). It is less time-consuming than histology and does not have the significant risks of biopsy, including haemorrhage, infection or visceral perforation [19].

Imaging techniques to be considered for diagnosing liver fibrosis in clinical practice include US or MRI elastography. Alternative methods for the evaluation of liver fibrosis are primarily of research interest and include: MRI with hepatobiliary contrast agents, T2-and T1-mapping techniques with quantitative MRI-derived extracellular volume (ECV) fraction, MR and CT perfusion, dual-energy CT, contrast-enhanced US (CEUS) and image texture analysis [20−26].

In schistosomiasis, the extent of liver fibrosis, as evaluated by MRI and liver histology, does not always relate to the clinical severity of portal hypertension because in some cases, even slight liver fibrosis is associated with severe portal hypertension. Several mediators can be involved in maintaining portal hypertension even after a decrease of liver fibrosis [27]. A promising approach in assessing liver fibrosis, has been proposed by Masi et al. who performed multiparametric MRI using quantitative T2 and T2* in an attempt to acquire quantitative values of early liver fibrosis, using a murine model of schistosomiasis where quantitative findings were compared to histological staging of liver disease and the grade of fibrosis progression [28].

The role of magnetic relaxation time parameters as markers of fibrosis has not yet been fully assessed, even though relaxometric studies have shown a good correlation between these parameters and liver fibrosis, without being specific for it. Guimares et al. demonstrated that the increase of T2 relaxation in liver fibrosis may be caused by inflammation associated with fibrogenesis [29].

MRI or CT techniques, specifically Magnetic Resonance Angiography (MRA) or Computed Tomography Angiography (CTA) may be used to create a vessels map, which may help to plan the best surgical approach for correction of portal hypertension.

The modalities of treatment of variceal bleeding in patients with schistosomiasis are varied and include medical options, such as the vasopressive substances also used in liver cirrhosis (beta-blockers), endoscopic approaches (sclerotherapy, band-ligation) or devascularization surgery (combinations of gastro-oesophageal devascularisation, surgical portal-systemic shunts and splenectomy). A TIPS procedure is an interventional treatment option for the complications of portal hypertension that commonly arise from liver cirrhosis, which offers an alternative to portosystemic shunt surgery in many settings

[30]. Although schistosomiasis may be a potential cause of non-cirrhotic portal hypertension, existing guidelines do not clearly indicate the use of TIPS procedures to treat the variceal bleeding that may occur in the late and advanced phase of schistosomiasis where there is liver involvement. Furthermore, there is a lack of consensus on the advantages of TIPS devices in schistosomiasis due to the potential risk of hepatic impairment secondary to reduction of portal pressures following device deployment. In comparison to surgery options, the TIPS procedure can be just as effective in controlling portal hypertension while being less invasive than open surgery and preserving the immunological role of the spleen. As observed by others [31], and also confirmed in our case, no evidence of liver impairment was documented and no signs or symptoms of encephalopathy were identified after 18 months of follow-up. Furthermore, MRI performed 18 months after the TIPS procedure, showed the regression of signal abnormalities due to periportal inflammation, suggesting its effectiveness as a treatment. We postulate that TIPS procedures may be superior to shunt surgery as it can be as effective in lowering portal hypertension while being less invasive than open surgery and maintaining the spleen in its immunological role.

4. Conclusion

Due to increased migratory flux from developing and endemic countries, radiologists should be familiar with the imaging appearance (US, CT and MRI) of hepatic schistosomiasis [32]. Imaging manifestations are only detectable late on in the natural course of disease. Chronic infection is also a risk factor for developing cirrhosis, complications of portal hypertension and hepatocellular carcinoma. Diagnostic imaging may replace invasive liver biopsy as a non-invasive diagnostic tool that can be used along with advanced imaging modalities, during the active surveillance of chronic disease. Interventional radiology may play an important role in the treatment of complications that arise in advanced disease.

Ethics statement

Informed consent from the patient for the case to be published (including images, case history and data) could not be obtained; exhaustive efforts were made to contact the patient over 6 months but proved unsuccessful. Patient data has been anonymised to protect the patient's identity.

Acknowledgement

References

[1] Meltzer E, Schwartz E. Schistosomiasis: current epidemiology and management. Travelers Curr Infect Dis Rep 2013;15:211−5.

[2] Leshem E, Maor Y, Meltzer E, Assous M, Schwartz E. Acute schistosomiasis outbreak: clinical features and economic impact. Clin Infect Dis 2008;47:1499−506.

[3] Muggli D, Müller MA, Karlo C, Fornaro J, Marincek B, Frauenfelder T. A simple method to approximate liver size on cross-sectional images using living liver models. Clin Radiol 2009;64:682−9.

[4] Kucybała I, Ciuk S, Tęczar J. Spleen enlargement assessment using computed tomography: which coefficient correlates the strongest with the real volume of the spleen? Abdom Radiol 2018;43:2455−61.

[5] Abdel-Wahab MF, Esmat G, Farrag A, El-Boraey YA, Strickland GT. Grading of hepatic schistosomiasis by the use of ultrasonography. Am J Trop Med Hyg 1992;46:403−8.

[6] Pinto-Silva RA, Queiroz LC, Azeredo LM, Silva LC, Lambertucci JR. Ultrasound in schistosomiasis mansoni. Mem Inst Oswaldo Cruz 2010; 105:479−84.

[7] Richter J, Domingues ALC, Barata CH, Prata AR, Lambertucci JR. Report of the second satellite symposium on ultrasound in schistosomiasis. Mem Inst Oswaldo Cruz 2001;96:151−6.

[8] Richter J, Monteiro ES, Braz RM, Abdalla M, Abdel-Rahim IM, Fano U, et al. Sonographic organometry in Brazilian and Sudanese patients with hepatosplenic Schistosomiasis mansoni and its relation to the risk of bleeding from oesophageal varices. Acta Trop 1992;51:281−90.

[9] Richter J, Dacal AR Corriea, Siqueira JG Vergetti, Poggensee G, Mannsmann U, Deelder A, et al. Sonographic prediction of variceal bleeding in patients with liver fibrosis due to Schistosoma mansoni. Trop Med Int Health 1998;3:728−35.

[10] Cota GF, Pinto-Silva RA, Antunes CM, Lambertucci JR. Ultrasound and clinical investigation of hepatosplenic schistosomiasis: evaluation of splenomegaly and liver fibrosis four years after mass chemotherapy with oxamniquine. Am J Trop Med Hyg 2006;74:103−7.

[11] Manzella A, Ohtomo K, Monzawa S, Lim JH. Schistosomiasis of the liver. Abdom Imag 2008;33:144−50.

[12] Bezerra ASA, D'Ippolito G, Caldana RP, Cecin AO, Ahmed M, Szejnfeld J. Chronic hepatosplenic schistosomiasis mansoni: magnetic resonance imaging and magnetic resonance angiography findings. Acta Radiol 2007;48:125−34.

[13] Semelka RC, Chung JJ, Hussain SM, Marcos HB, Woosley JT. Chronic hepatitis: correlation of early patchy and late linear enhancement patterns on gadolinium-enhanced MR images with histopathology initial experience. J Magn Reson Imag 2001;13:385−91.

[14] Brancatelli G, Federle MP, Grazioli L, Golfieri R, Lencioni R. Large regenerative nodules in Budd-Chiari syndrome and other vascular disorders of the liver: CT and MR imaging findings with clinicopathologic correlation. AJR Am J Roentgenol 2002;178:877−83.

[15] Goshima S, Kanematsu M, Watanabe H, Kondo H, Kawada H, Moriyama N, et al. Gd-EOBDTPA-enhanced MR imaging: prediction of hepatic fibrosis stages using liver contrast enhancement index and liver-to-spleen volumetric ratio. J Magn Reson Imag 2012;36:1148−53.

[16] Annet L, Peeters F, Abarca-Quinones J, Leclercq I, Moulin P, Van Beers BE. Assessment of diffusion-weighted MR imaging in liver fibrosis. J Magn Reson Imag 2007;25:122−8.

[17] Fu F, Li X, Chen C, Bai Y, Liu Q, Shi D, et al. Non-invasive assessment of hepatic fibrosis: comparison of MR elastography to transient elastography and intravoxel incoherent motion diffusion-weighted MRI. Abdom Radiol (NY) 2020;45:73−82.

[18] Jiang H, Chen J, Gao R, Huang Z, Wu M, Song B. Liver fibrosis staging with diffusion-weighted imaging: a systematic review and meta-analysis. Abdom Radiol (NY) 2017;42:490−501.

[19] Li YT, Cercueil JP, Yuan J, Chen W, Loffroy R, Wáng YX. Liver intravoxel incoherent motion (IVIM) magnetic resonance imaging: a comprehensive review of published data on normal values and applications for fibrosis and tumor evaluation. Quant Imag Med Surg 2017;7: 59−78.

[20] Voieta I, de Queiroz LC, Andrade LM, Silva LC, Fontes VF, Barbosa Jr A, et al. Imaging techniques and histology in the evaluation of liver fibrosis in hepatosplenic schistosomiasis mansoni in Brazil: a comparative study. Mem Inst Oswaldo Cruz 2010;105:414−21.

[21] Luetkens JA, Klein S, Träber F, Block W, Schmeel FC, Sprinkart AM, et al. Quantification of liver fibrosis: extracellular volume fraction using an MRI bolus-only technique in a rat animal model. Eur Radiol Exp 2019;3:22.

[22] Venkatesh SK, Wang G, Lim SG, Wee A. Magnetic resonance elastography for the detection and staging of liver fibrosis in chronic hepatitis B. Eur Radiol 2014;24:70−8.

[23] Chen BB, Hsu CY, Yu CW, Wei SY, Kao JH, Lee HS, et al. Dynamic contrast-enhanced magnetic resonance imaging with Gd-EOB-DTPA for the evaluation of liver fibrosis in chronic hepatitis patients. Eur Radiol 2012;22:171−80.

[24] Guo SL, Su LN, Zhai YN, Chirume WM, Lei JQ, Zhang H, et al. The clinical value of hepatic extracellular volume fraction using routine multiphasic contrast-enhanced liver CT for staging liver fibrosis. Clin Radiol 2017;72:242−6.

[25] Lamb P, Sahani DV, Fuentes-Orrego JM, Patino M, Ghosh A, Mendonca PR. Stratification of patients with liver fibrosis using dual-energy CT. IEEE Trans Med Imag 2015;34:807−15.

[26] Van Beers BE, Leconte I, Materne R, Smith AM, Jamart J, Horsmans Y. Hepatic perfusion parameters in chronic liver disease: dynamic CT measurements correlated with disease severity. AJR Am J Roentgenol 2001;176:667−73.

[27] Bosch J, Groszmann R, Shah VH. Evolution in the understanding of the pathophysiological basis of portal hypertension: how changes in paradigm are leading to successful new treatments. J Pathol 2015;62: S121−30.

[28] Masi B, Perles-Barbacaru TA, Laprie C, Dessein H, Bernard M, Dessein A, et al. In vivo MRI assessment of hepatic and splenic disease in a murine model of schistosomiasis. PLoS Neglected Trop Dis 2015;16: e0004036.

[29] Guimaraes AR, Siqueira L, Uppal R, Alford J, Fuchs BC, Yamada S, et al. T2 relaxation time is related to liver fibrosis severity. Quant Imag Med Surg 2016;6:103−14.

[30] Boyer TD, Haskal ZJ. American Association for the Study of Liver Diseases. The role of transjugular intrahepatic portosystemic shunt (TIPS) in the management of portal hypertension: update 2009. Hepatology 2010;51:306.

[31] Richter J, Bode JG, Blondin D, Kircheis G, Kubitz R, Holtfreter MC, et al. Severe liver fibrosis caused by Schistosoma mansoni: management and treatment with a transjugular intrahepatic portosystemic shunt. Lancet Infect Dis 2015;15:731−7.

[32] Masi B, Perles-Barbacaru TA, Bernard M, Viola A. Clinical and preclinical imaging of hepatosplenic schistosomiasis. Trends Parasitol 2020 Feb;36(2):206−26.